Hindawi Publishing Corporation
International Journal of Photoenergy
Volume 2015, Article ID 497697, 13 pages
http://dx.doi.org/10.1155/2015/497697

Research Article

Coordinated Control of PV Generation and EVs Charging Based on Improved DECell Algorithm

Guo Zhao,[1,2] Xueliang Huang,[1,2] and Hao Qiang[1,3]

[1]*School of Electrical Engineering, Southeast University, Nanjing 210096, China*
[2]*Jiangsu Key Lab of Smart Grid Technology and Equipment, Zhenjiang 212009, China*
[3]*School of Urban Rail Transit, Changzhou University, Changzhou 213164, China*

Correspondence should be addressed to Guo Zhao; zhaoguoabc@126.com

Received 25 September 2014; Revised 30 December 2014; Accepted 30 December 2014

Academic Editor: Zhixiong Guo

Recently, the coordination of EVs' charging and renewable energy has become a hot research all around the globe. Considering the requirements of EV owner and the influence of the PV output fluctuation on the power grid, a three-objective optimization model was established by controlling the EVs charging power during charging process. By integrating the meshing method into differential evolution cellular (DECell) genetic algorithm, an improved differential evolution cellular (IDECell) genetic algorithm was presented to solve the multiobjective optimization model. Compared to the NSGA-II and DECell, the IDECell algorithm showed better performance in the convergence and uniform distribution. Furthermore, the IDECell algorithm was applied to obtain the Pareto front of nondominated solutions. Followed by the normalized sorting of the nondominated solutions, the optimal solution was chosen to arrive at the optimized coordinated control strategy of PV generation and EVs charging. Compared to typical charging pattern, the optimized charging pattern could reduce the fluctuations of PV generation output power, satisfy the demand of EVs charging quantity, and save the total charging cost.

1. Introduction

With the increasing pressures of energy shortage, environmental pollution, and global warming, the developments of renewable energies such as wind power and photovoltaic (PV) generation [1, 2] have been paid more and more attention. In addition, for the purposes of low-carbon emissions and reducing environmental pollution, the electric vehicle (EV) technology also obtained fast development and now has become a focus of national governments, automakers, and energy companies [3–6]. However, research shows that EVs' advantage of low emissions is more significant only in predominant low-carbon electricity area, while it is not obvious in the region based on coal-fired power generation. This means that only as much as possible wind power, PV power, and other renewable energies are adopted to charge the EVs, can EVs' emission reduction benefits be full play. Therefore, the coordination and complementation of EVs' charging and wind power or PV power have become a hot research all around the globe [7–12].

Recently, most research has focused on the coordination of EVs and renewable energy based on the coordination scheduling and EVs charging station's capacity allocation. Paper [13] derived the mathematical expectation analytical expressions of wind turbines outputs and EVs in the state of the V2G; based on this, a power system stochastic economic dispatch model was developed for the target of minimization of total generation cost. Paper [14] did research on output probability distribution of V2G, wind power, and PV generation system, set up a stochastic optimization scheduling model to stabilize the fluctuations of renewable energy outputs, and solved the model by the cross entropy algorithm. Paper [15] established a multiobjective optimization model for EV charging to decrease the equivalent load peak valley difference and regional grid electricity purchasing cost, then transformed multiobjective optimization model into a single objective optimization problem by fuzzy set theory, and adopted an improved particle swarm algorithm to solve the model. Paper [16] established a capacity optimization model of the PV charging station to minimize the system

comprehensive cost and maximize the utilization of renewable energy. While the cost of EVs charging and the influences on the power grid are rarely simultaneously considered, this issue is practically valuable to EVs development.

Considering the requirements of EV owner and the influence of the PV output fluctuation on the power grid, the issue of coordination of EVs and renewable energy would become a multiobjective optimization problem. A three-objective optimization model of PV generation and EV charging system, including minimum cost, full state of charge, and minimal fluctuation of PV output power, has been proposed.

In order to solve the established three-objective optimization model, an effective multiobjective optimization algorithm is needed. In recent years, many classical multiobjective evolutionary algorithms had emerged, such as NSGA-II [17] and Strength Pareto Evolutionary Algorithm II (SPEA2) [18]. In 2007, Enrique Alba developed a novel multiobjective cellular genetic algorithm (cMOGA). Later, Nebro et al. improved the cMOGA by introducing a feedback mechanism, thus forming an improved cMOGA, that is, MOCell [19]. Pareto solution obtained by MOCell has outstanding uniformity when solving the double target problem, while it is disappointing in the three target problems. In order to improve the performance of MOCell, Durillo et al. combined differential evolution (DE) algorithm with the MOCell and proposed a hybrid metaheuristic algorithm DECell [20]. At present, the DECell algorithm has been applied in the practical engineering problems and achieved good effects [21].

For further improvement of DECell algorithm's performance in solving multiobjective optimization problem, meshing method [22] is integrated into the basic DECell algorithm and acquired an improved DECell (IDECell) algorithm. Through solving the multiobjective benchmark functions, it is verified that IDECell algorithm is effective and feasible which can obtain more uniform distribution of Pareto front compared to NSGA-II and basic DECell algorithm. Finally, an optimized control strategy for coordinated control of PV generation and EVs charging could be chosen by normalized sorting of the nondominated solutions. Compared to typical charging pattern, the optimized charging pattern could reduce the fluctuations of PV generation output power, meet the demand of EVs' charging, and save the total charging cost.

2. The Coordination Optimization Model of PV Generation and EVs Charging

The main types of EVs are bus, taxi and private car, and so forth. Their charging patterns are divided into slow charging, conventional charging, and fast charging. Among them, private cars are mainly used for work, leisure, and entertainment; the corresponding charging locations include office parking lot, residential parking lot, and supermarket shopping center parking lot. Therefore, the charging patterns could be chosen as slow charging or conventional charging when parking in the office and residential parking lots. In this paper, the private cars charging in the office parking lot condition is taken as an example to study the coordinated optimization control strategy of PV generation and EVs charging, and the charging time is from when they arrive at work locations to when they leave.

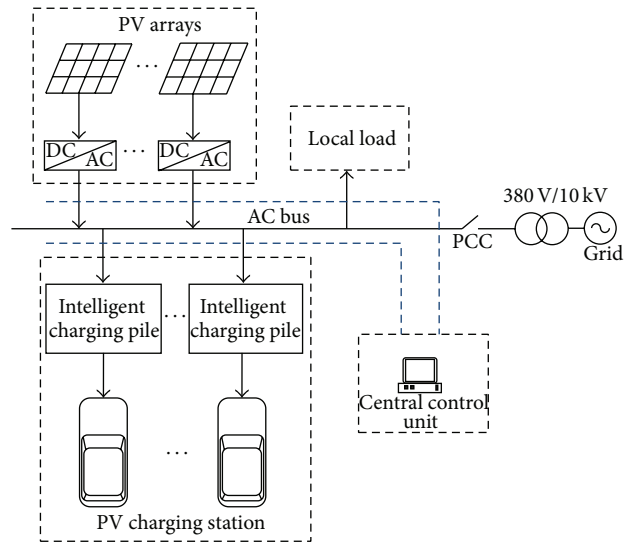

Figure 1: Structure of the PV charging station system.

2.1. Power Balance Model of PV Charging Station System. The PV charging station researched in this paper is comprised of PV arrays, DC/AC modules, intelligent charging piles, local load, AC power source, and central control unit; the system structure is as shown in Figure 1.

Under stable operation condition of the PV charging station system, the tie line power is considered to be grid connected power which can be calculated by the following:

$$P_{gs} = P_{PV} - P_{EV} - P_{loss}, \tag{1}$$

where P_{gs} is the power transmitted to the grid, P_{PV} is the output power of PV generation system, P_{EV} is the total consumed power of EVs charging, and P_{loss} is the loss power of lines. Besides, all values of the variables above are instantaneous values.

2.2. Objective Functions

(1) Fluctuations of the Power Transmitted to the Grid. In order to investigate the optimal control strategy for coordinated charging, the whole optimization period T is divided equally into N sections, and the duration T_N of each section can be derived as T/N.

To reduce the influence of grid connected PV generation on the power grid side, it is needed to minimize the fluctuations of the power transmitted to the grid through the optimal control of EVs' charging power of each section in the charging process. Use standard deviation to estimate the fluctuation characteristic of the power transmitted to the grid. Then the corresponding objective function can be expressed as

$$\min F_1 = \min \sqrt{\frac{\sum_{n=1}^{N} \left| P_{gs}(n) - \overline{P}_{gs} \right|^2}{N}}, \tag{2}$$

where $P_{gs}(n) = P_{PV}(n) - \sum_i^{num\_EV} P_{EV}(n,i)$ is the average value of power transmitted to the grid during the nth section; $\overline{P}_{gs} = \sum_{n=1}^{N}[P_{PV}(n) - \sum_i^{num\_EV} P_{EV}(n,i)]/N$ is the average value of power transmitted to the grid during the whole optimization period; $P_{PV}(n)$ is the average value of PV generation output power during the nth section; $P_{EV}(n,i)$ represents the average charging power of ith EV during nth section; num_EV is the total number of EV battery chargers.

(2) EVs Charging Cost. According to TOU price of industrial electricity in China, the cost of EV charging can be calculated by the following:

$$\text{cost} = \int_{t_0}^{t_0+T} M(t)\,P(t)\,dt, \tag{3}$$

where t_0 is the starting time of charging, T is duration of charging, and $t_0 + T$ is the ending time of charging. $M(t)$ and $P(t)$ represent the unit price and charging power in time t, respectively. Take the total cost that all EVs need to pay to charge as objection function:

$$\min F_2 = \min \sum_{n=1}^{N} M(n) \sum_{i}^{num\_EV} P_{EV}(n,i)\,T_N. \tag{4}$$

(3) SOC of EV Battery. The SOC of EV battery can be stated as

$$\text{SOC}(t) = \text{SOC}_0 + \frac{\int_{t_0}^{t_0+T} P(t)\,dt}{Q}, \tag{5}$$

where SOC_0 represents the initial SOC of EV battery and Q is the rated capacity of EV battery. After being discretized, (5) can be rewritten as

$$\text{SOC}(n) = \text{SOC}_0 + \frac{\sum_{j=1}^{n} P(j)\,T_N}{Q}. \tag{6}$$

In order to satisfy the user's charging requirements, the EV battery should be fully charged at the end of the optimization. The discretized optimized model can be expressed as

$$\min F_3 = \min \sum_{i}^{num\_EV} |\text{SOC}(N,i) - 1|^2. \tag{7}$$

2.3. Constraints

(1) Restriction of the Power Transmitted to the Grid. Consider

$$P_{gs\,min} \le P_{gs}(n) \le P_{gs\,max}, \tag{8}$$

where $P_{gs\,min}$ and $P_{gs\,max}$ represent the minimum value and maximum value of grid connected power, respectively, which can be confirmed according to the agreement between PV charging station system and power grid.

(2) Restriction of Charging Power. In order to reduce the life loss of EV battery, the charging power of EV battery should not exceed a certain limited value. The charging power is constrained by the following:

$$0 < P(t) \le P_{charge\,max}(t), \tag{9}$$

where $P_{charge\,max}(t)$ represents the maximum acceptable charging power of EV battery in time t, which is the function of SOC and temperature of battery. Temperature effect on $P_{charge\_max}(t)$ can be ignored when some measures are taken to keep the temperature of battery constant. Then the maximum acceptable charging power can be expressed as follows:

$$P_{charge\,max}(t) = f(\text{SOC}). \tag{10}$$

The quantitative relationship between $P_{charge\,max}(t)$ and SOC can be described by SOC curve which is shown in Figure 2.

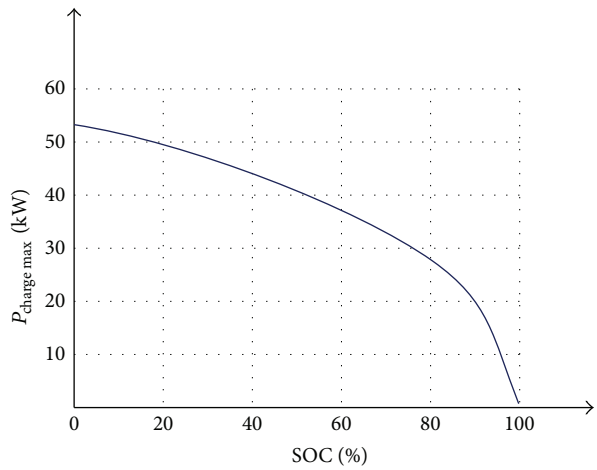

Figure 2: The SOC curve.

Except for the restriction $P_{charge\,max}(t)$ which is the maximum acceptable charging power of EV battery, the total charging power of all EVs in each section of the charging period is also restricted by the following:

$$\sum_{i}^{num\_EV} P_{EV}(n,i) \le P_{PV}(n). \tag{11}$$

(3) Restriction of EV Battery's SOC. The SOC of EV battery in each section of the charging period should be restricted by the following:

$$\begin{aligned} &\text{SOC}(n+1) = \text{SOC}(n) + \frac{P(n)\,T_N}{Q}, \\ &\text{SOC}_0 \le \text{SOC}(n) \le 1, \quad n = 1, 2, \ldots, N. \end{aligned} \tag{12}$$

2.4. Three-Objective Optimization Model. Based on the above formulas, the global optimization of the coordinated control

of PV generation and EVs charging can be expressed as a three-objective optimization problem with constraints:

$$\begin{aligned}
&\min F_1 = \min \sqrt{\frac{\sum_{n=1}^{N} \left|P_{\text{gs}}(n) - \overline{P}_{\text{gs}}\right|^2}{N}}, \\
&\min F_2 = \min \sum_{n=1}^{N} M(n) \sum_{i}^{\text{num_EV}} P_{\text{EV}}(n,i)\, T_N, \\
&\min F_3 = \min \sum_{i}^{\text{num_EV}} \left|\text{SOC}(N,i) - 1\right|^2,
\end{aligned} \tag{13}$$

$$\begin{aligned}
\text{S.T.} \quad & P_{\text{gs min}} \le P_{\text{gs}}(n) \le P_{\text{gs max}} \\
& 0 < P(t) \le P_{\text{charge max}}(t) \\
& \sum_{i}^{\text{num_EV}} P_{\text{EV}}(n,i) \le P_{\text{PV}}(n) \\
& \text{SOC}(n+1) = \text{SOC}(n) + \frac{P(n)\, T_N}{\text{Q}} \\
& \text{SOC}_0 \le \text{SOC}(n) \le 1, \quad n = 1, 2, \ldots, N.
\end{aligned} \tag{14}$$

3. IDECell Algorithm

3.1. Basic DECell Algorithm. DECell is an improved multiobjective optimization algorithm based on MOCell algorithm; the basic idea is to use MOCell as a search engine and then use the propagation mechanism of differential evolution (DE) instead of the crossover operating and mutation operating of traditional genetic algorithm to generate new individuals, so that the Pareto front of solution set can be obtained in maintaining good uniformity and distribution breadth, while moving closer and closer to the optimal front.

(1) Basic Principle of DECell Algorithm. The basic principle chart of DECell algorithm is as shown in Figure 3. Firstly, an initial population is generated randomly and an external empty document for Pareto solution set is also generated, and then individuals of the initial population will be placed in a two-dimensional ring network and the neighbor structure type could be defined too. Secondly, two different individuals will be selected from the neighbors of each current individual randomly to constitute the three male parent individuals; then crossover operating and mutation operating of the DE strategy will be carried out to produce an offspring individual. If the offspring individual dominates the current parent individual or the offspring individual has greater crowding distance while both of them are nondominated, replace the current parent individual with the offspring individual and store it to the external document. Calculate the crowding distance of each nondominated individual in the external document and delete the individual which has the minimum crowding distance when the quantity of the external document exceeds its specified capacity. Finally, after the completion of each iteration, select a number of individuals from the external document to replace the same number of individuals randomly selected from current population so that the population could be updated constantly by this feedback mechanism. As a result, the Pareto front of obtained solution set can keep the diversity, while moving closer and closer to the optimal front.

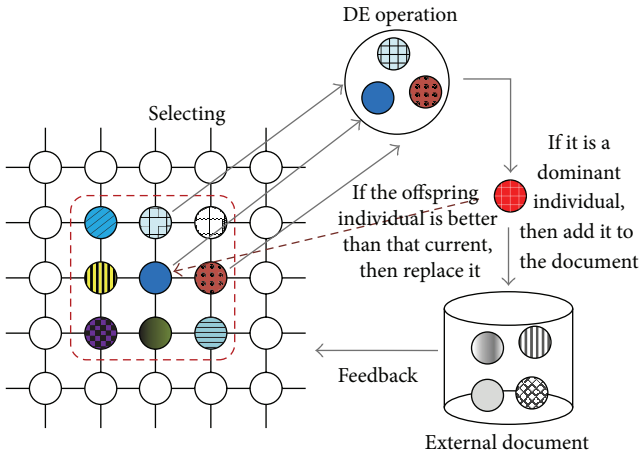

Figure 3: Basic principle chart of DECell algorithm.

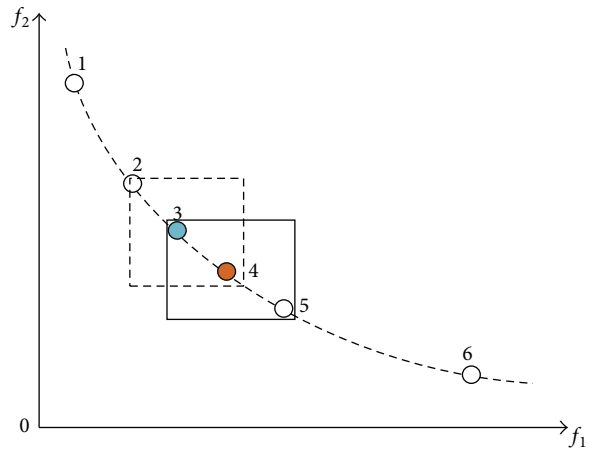

Figure 4: Crowding distances of individual 3 and individual 4.

(2) The Deficiency of Crowding Distance Strategy in DECell Algorithm. In DECell algorithm, the crowding distance strategy is used to keep the solution set's diversity; the crowding distance of each individual of each evolution population is calculated and the individual with great crowding distance value has the priority to be selected into the next generation population. However, the limitation of this strategy is that some individuals with good distribution may be eliminated while those with bad distribution may be reserved.

As shown in Figure 4, individual 3 and individual 4 are adjacent and both of them are relatively far from other individuals; in this case, their crowding distance values are relatively great and similar. Therefore, individual 3 and

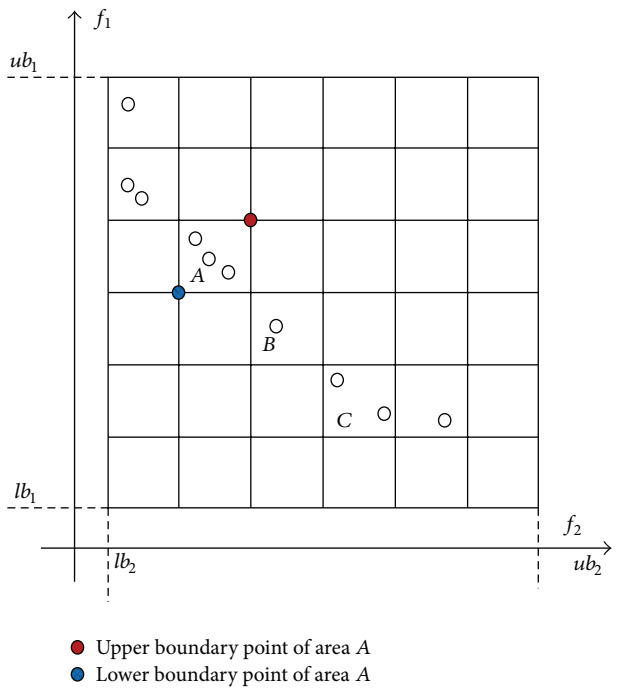

FIGURE 5: Mesh and its boundaries.

individual 4 will be eliminated or reserved simultaneously. However, in order to make the solution population maintain good uniformity and distribution, it is better to reserve one and eliminate the other from individual 3 and 4. In view of this problem, meshing method will be introduced to improve the performance of DECell algorithm instead of the crowding distance strategy.

3.2. Meshing Method. For a r-objective optimization problem, set a grid with $2r$ boundaries. lb_k and ub_k are the according lower and upper boundary, respectively, where $k = 1, 2, \ldots, r$. That shown in Figure 5 is a 2-objective grid with 4 boundaries in total.

A grid can be segmented into several small areas called hypercube (HC); the amount of segmentation depends on the size of evolution population and the objective number of the optimization problem. Each HC could be expressed as r^i, where $i = (i_1, i_2, \ldots, i_r)$; besides, $i_k \in 1 \cdots d$, where d is a natural constant generally greater than 2 which represents the amount of segmentation in each dimension. In Figure 5, d is set as 6; therefore, boundaries of each r^i can be expressed as

$$\forall k \in 1 \cdots r,$$

$$rub_{k,i} = \left[lb_k + \left(\frac{i_k}{d}\right)(ub_k - lb_k)\right] \cdot \omega_k, \quad (15)$$

$$rlb_{k,i} = \left[lb_k + \left(\frac{(i_k - 1)}{d}\right)(ub_k - lb_k)\right] \cdot \omega_k,$$

where ω_k represents the width of each HC in kth dimension, $\omega_k = \text{range}_k/d$, and range_k is the domain width in kth dimension.

On the basis of the above, with the grid and the identification for each HC, it can be judged whether an individual falls in a certain area. Take individual $z = (z_1, z_2, \ldots, z_r)$, for instance; it can be confirmed that individual z is located in area r^i when $z_k \geq rlb_{k,i}$ and $z_k < rub_{k,i}$, $\forall k \in 1 \cdots r$.

In Figure 5, there are three individuals located in area A, one individual located in area B, and two individuals located in area C. To maintain the evolution population's distribution, it is needed to select the individuals with great gathering density in the grid to delete. Therefore, one or two individuals in the area A should be deleted.

3.3. Improvement of DECell Algorithm. In order to improve the performance of DECell algorithm solving the three-objective optimization problem, meshing method is integrated into the basic DECell algorithm instead of the crowding distance strategy. As a result, an improved differential evolution cellular (IDECell) genetic algorithm was developed. The flowchart of IDECell algorithm is as shown in Figure 6.

3.4. Verification of IDECell Algorithm. In order to verify the feasibility of IDECell algorithm, apply IDECell algorithm to solve two three-objective benchmark test functions DTLZ1 and DTLZ2. What is more, NSGA-II algorithm and basic DECell algorithm are also conducted for comparison. DTLZ1 and DTLZ2 are described as (16) and (17), respectively:

DTLZ1:

$$\begin{aligned}
&\min f_1(x) = 0.5x_1x_2(1 + g(x))\\
&\min f_2(x) = 0.5x_1(1 - x_2)(1 + g(x))\\
&\min f_3(x) = 0.5(1 - x_1)(1 + g(x))\\
&g(x) = \sum_{i=3}^{12}(x_i - 0.5)^2 - \cos(20\pi(x_i - 0.5))\\
&\text{S.T.} \quad 0 \leq x_i \leq 1 \quad (i = 1, 2, \ldots, 12),
\end{aligned} \quad (16)$$

DTLZ2:

$$\begin{aligned}
&\min f_1(x) = (1 + g(x))\cos\left(x_1\frac{\pi}{2}\right)\cos\left(x_2\frac{\pi}{2}\right)\\
&\min f_2(x) = (1 + g(x))\cos\left(x_1\frac{\pi}{2}\right)\sin\left(x_2\frac{\pi}{2}\right)\\
&\min f_3(x) = (1 + g(x))\sin\left(x_1\frac{\pi}{2}\right)\\
&g(x) = \sum_{i=3}^{12}(x_i - 0.5)^2\\
&\text{S.T.} \quad 0 \leq x_i \leq 1 \quad (i = 1, 2, \ldots, 12).
\end{aligned} \quad (17)$$

3.4.1. Performance Measures. Unlike in single objective optimization, there are two goals in a multiobjective optimization: (1) convergence to the Pareto-optimal set and (2) maintenance of diversity in solutions of the Pareto-optimal

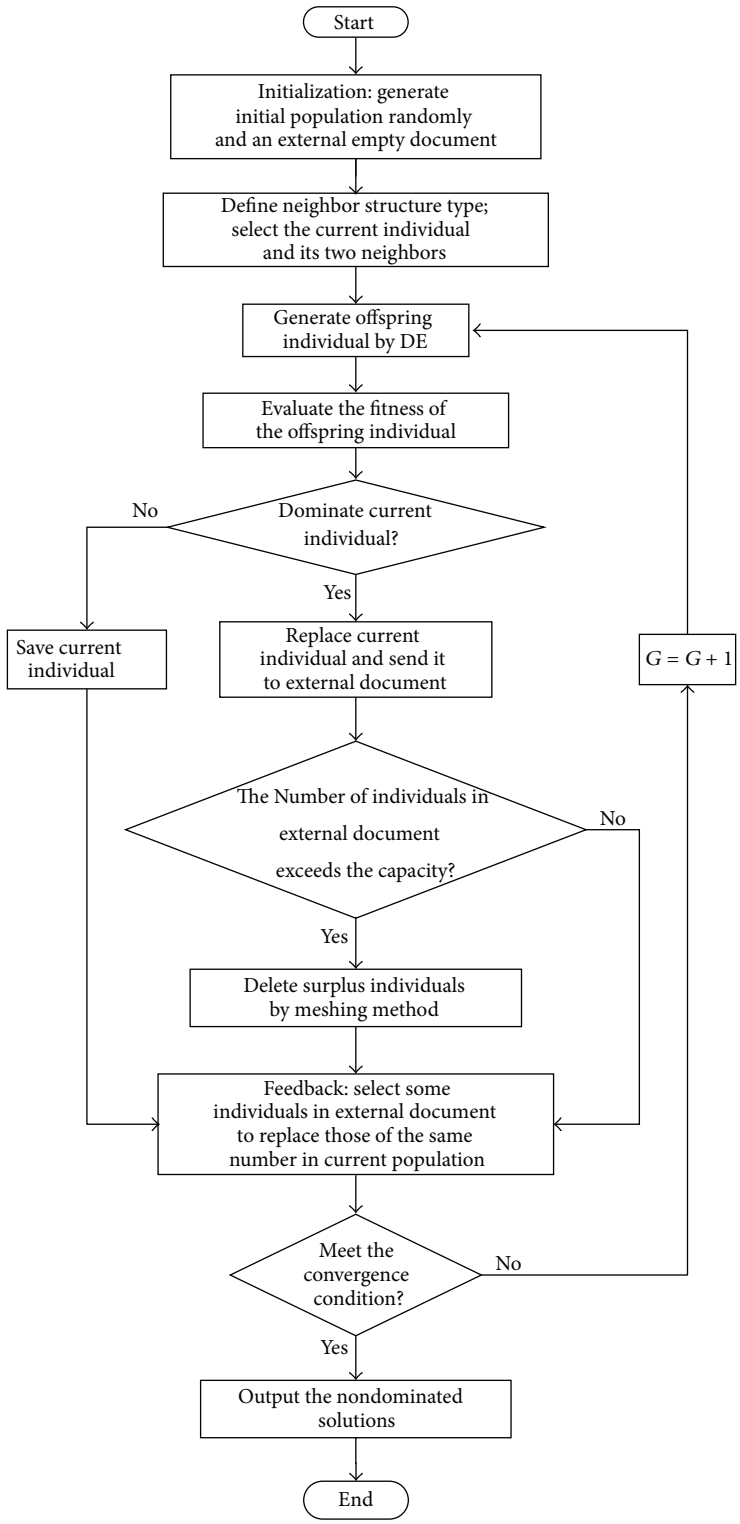

Figure 6: The flowchart of IDECell algorithm.

set [23]. These two tasks cannot be measured adequately with one performance metric. Many performance metrics have been suggested [17, 24, 25]. Here, we use three practical performance metrics to evaluate the above two goals in a solution set obtained by a multiobjective optimization algorithm.

(1) Generational Distance. This metric is a value representing the distance between the obtained Pareto front and the optimal Pareto front and is defined as [24]

$$\mathrm{GD} = \frac{\left(\sum_{i=1}^{n} d_i^p\right)^{1/p}}{n}, \tag{18}$$

where n is the number of solutions in the obtained Pareto front, p is the dimension of objective space, and d_i is the Euclidean distance between each solution and the nearest member of the optimal Pareto front. A result of 0 indicates that the obtained Pareto front is optimal Pareto front. The metric GD takes a smaller value with better performance in convergence.

(2) Spread, Δ. The metric Δ suggested by Deb et al. measures the extent of spread achieved among the obtained solutions [17]. We use this metric to calculate the nonuniformity in the distribution:

$$\Delta = \frac{d_f + d_l + \sum_{i=1}^{n} \left| d_i - \overline{d} \right|}{d_f + d_l + (n-1) \times \overline{d}}. \tag{19}$$

Here, d_i is Euclidean distance between consecutive solutions in the obtained nondominated set of solutions. The parameters d_f and d_l are the Euclidean distances between the extreme solutions and the boundary solutions of the obtained nondominated set. The parameter $\overline{d}$ is the average of all distances d_i, assuming that there are n solutions on the best nondominated front. The metric Δ takes a higher value with worse distributions of solutions within the extreme solutions.

(3) Hypervolume. Hypervolume (HV) metric [25] is used to represent the volume of the objective space dominated by an approximation Pareto set. It is a comprehensive evaluation indicator of convergence and diversity and is defined as

$$\mathrm{HV} = \mathrm{volume}\left(\bigcup_{i=1}^{|Q|} v_i\right), \tag{20}$$

where Q is the number of solutions in the obtained Pareto front. For each individual, V_i represents the volume dominated by the ith individual and the reference point $w = (0, \ldots, 0)$. The greater value of the HV shows that the obtained Pareto front has wider coverage in the optimal Pareto front.

3.4.2. Analysis of the Results. Set the parameters of three algorithms as follows: adopt real number system for encoding and polynomial for mutation. NSGA-II adopts simulation binary crossover (SBX) operator; DECell and IDECell adopt DE operator. Population size is set as 200, the maximum

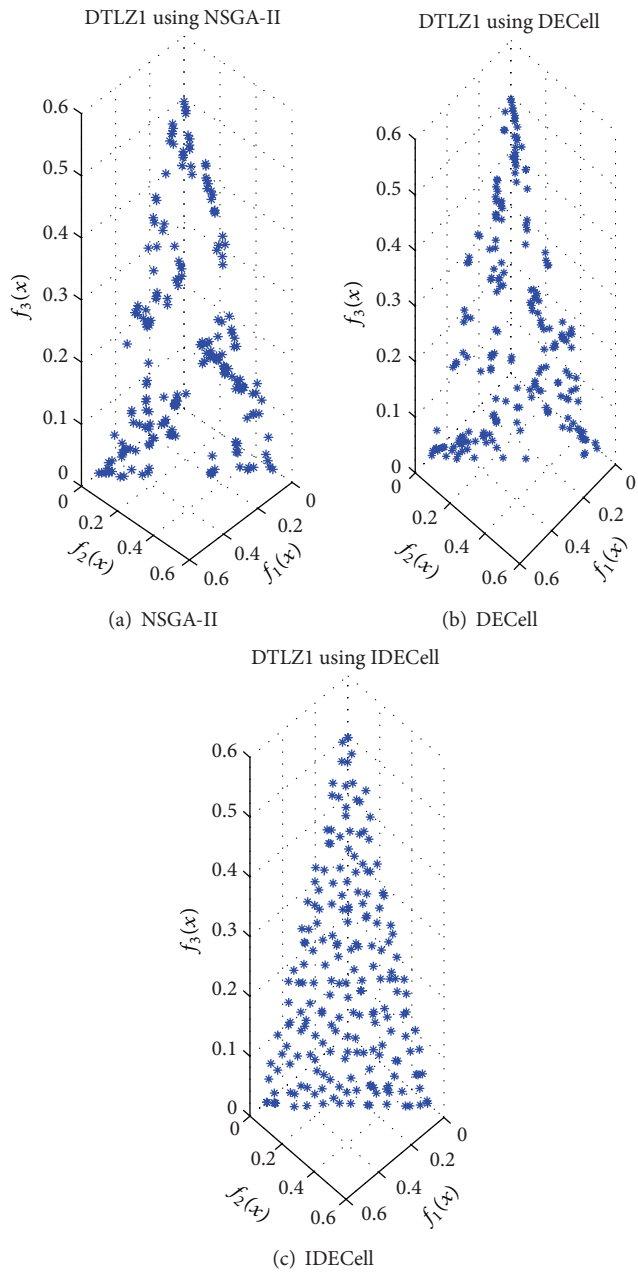

(a) NSGA-II (b) DECell

(c) IDECell

Figure 7: Pareto front of DTLZ1 gained by 3 multiobjective optimization algorithms.

number of iterations is set as 1000, crossover probability is set as 0.9, mutation probability is 1/len, len is variable dimension, the size of external document is set as 100, and the number of feedback individuals is set to be 20. Altogether 30 independent runs were performed per algorithm and test problem in order to restrict the influence of random effects. The simulation results gained by three optimization algorithms are shown as Figures 7 and 8.

Obviously, it can be seen from Figures 7 and 8; all three algorithms can seek out a group of nondominated solutions for DTLZ1 and DTLZ2. Compared to other two optimization algorithms, the Pareto front gained by IDECell algorithm has

Table 1: Comparison of performance metrics.

Algorithm (problem)	GD		Δ		HV	
	Mean	Variance	Mean	Variance	Mean	Variance
NSGA-II (DTLZ1)	0.2036	0.1601	0.8651	0.0262	0.7221	0.0471
DECell (DTLZ1)	0.0424	0.0427	0.6978	0.0145	0.7862	0.0524
IDECell (DTLZ1)	0.0233	0.0607	0.5034	0.0092	0.8025	0.0413
NSGA-II (DTLZ2)	0.2263	0.4644	0.9552	0.1227	0.6343	0.0793
DECell (DTLZ2)	0.0196	0.0241	0.8987	0.2475	0.7064	0.0617
IDECell (DTLZ2)	0.0177	0.0221	0.4954	0.0178	0.7285	0.0814

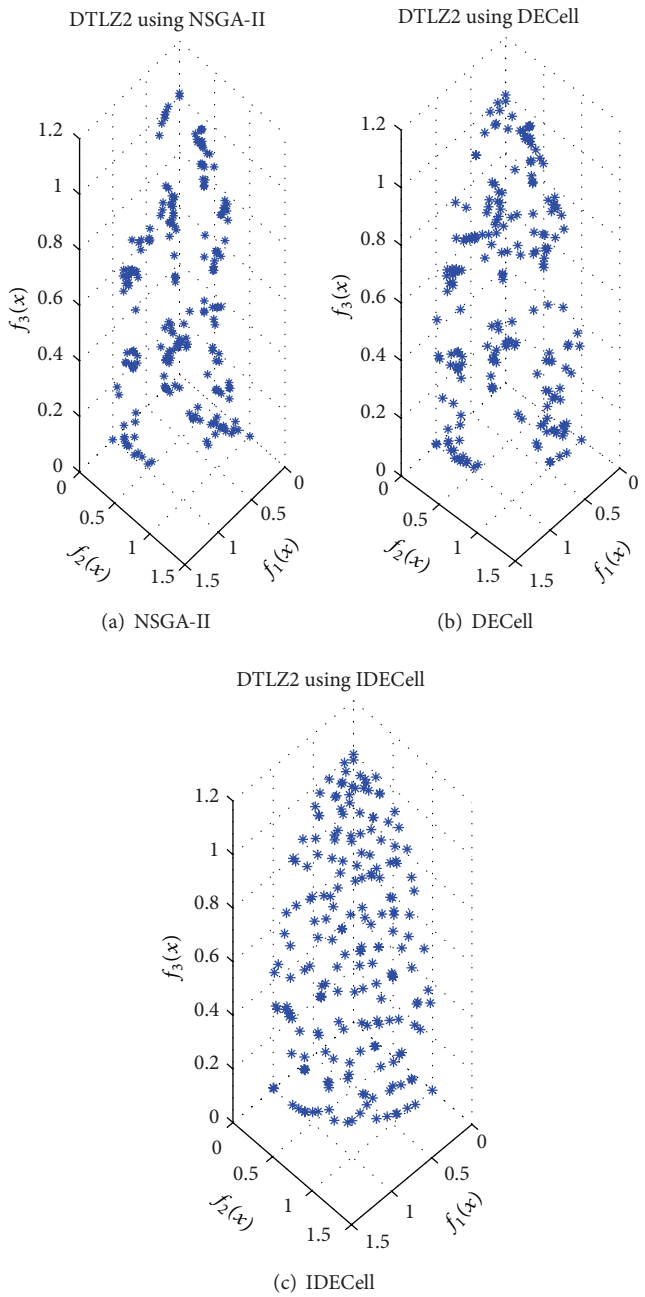

(a) NSGA-II (b) DECell

(c) IDECell

Figure 8: Pareto front of DTLZ2 gained by 3 multiobjective optimization algorithms.

more uniform distribution. The case that multiple optimal solutions converge in a small area does not exist, avoiding the premature and local convergence during the process of genetic operation. Furthermore, quality measures have been introduced to compare the outcomes of multiobjective optimization algorithms in a quantitative manner. Table 1 presents three algorithms performance as regards generational distance, spread, and hypervolume over DTLZ1 and DTLZ2. When considering generational distance and hypervolume, the DECell algorithm and IDECell algorithm give better results than the NSGA-II algorithm because they combine the advantages of MOCell algorithm and DE algorithm. Besides, due to the introduction of the meshing method, the IDECell algorithm shows better performance in the uniform distribution than the other two algorithms over the test problems. As such, it is verified that the IDECell algorithm is more suitable and reliable to solve the three-objective optimization problem and is advantageous for policy makers to accurately make the best choice.

4. Application of IDECell Algorithm in the Coordinated Control of PV Generation and EVs Charging

Apply the IDECell algorithm to solve the established optimization model for the coordinated control of PV generation and EVs charging; the overall process can be described in the following main steps.

Step 1 (initialize the parameters). Set the parameters of P, N_D, F, CR, d, C, and G. P is the population size. N_D represents the size of external document. F is the zoom factor. CR is the crossover factor. d is the amount of segmentation. C is the number of feedback individuals and G is the maximum number of iterations for whole population.

Step 2 (initialize the population randomly). Generate the initial population randomly meeting the constraints described in (14): $X_1, X_2, \ldots, X_P$, $X_i = (P_{\mathrm{EV}}(1,i), P_{\mathrm{EV}}(2,i), \ldots, P_{\mathrm{EV}}(N,i))$, and generate an empty external document as well. Then place the individuals of the initial population in a two-dimensional ring network and its neighbor structure type could be defined as Moore. Compute the fitness value $[F_1(X_i), F_2(X_i), F_3(X_i)]$ according to (13) for each individual X_i.

Step 3 (generate the offspring individuals by DE). For each individual of current population, select two individuals $X_{r2,G}$

and $X_{r3,G}$ from all neighbors of the current individual $X_{r1,G}$. $r1$, $r2$, and $r3$ are their index position, respectively. A new individual can be obtained by crossover operation according to (21): $V_{i,G} = (v_{i,1,G}, v_{i,2,G}, \ldots, v_{i,j,G}, \ldots, v_{i,N,G})$; then, to its paternal individual $X_{i,G} = (x_{i,1,G}, x_{i,2,G}, \ldots, x_{i,j,G}, \ldots, x_{i,N,G})$, carry out the mutation operation according to (22) to get the new offspring individual, $U_{i,G+1} = [u_{i,1,G+1}, u_{i,2,G+1}, \ldots, u_{i,j,G+1}, \ldots, u_{i,N,G+1}]$:

$$V_{i,G} = X_{r1,G} + F \cdot \left(X_{r2,G} - X_{r3,G}\right), \tag{21}$$

$$u_{i,j,G+1} = \begin{cases} v_{i,j,G}, & \text{rand}_j < \text{CR or } j = K; \\ x_{i,j,G}, & \text{others}, \end{cases} \tag{22}$$

where K is a integer and $0 \leqslant K \leqslant N - 1$.

Step 4 (evaluate the offspring individuals). Compute the fitness value $[F_1(U_{i,G+1}), F_2(U_{i,G+1}), F_3(U_{i,G+1})]$ according to (13) for offspring individual $U_{i,G+1}$. If $U_{i,G+1}$ dominates its paternal individual $X_{i,G}$, then replace the paternal individual and send $U_{i,G+1}$ to the external document.

Step 5 (feedback). Sort the nondominated individuals stored in the external document using meshing method and delete the redundant individuals when the quantity of the document exceeds its specified capacity. Select a number of individuals from the external document to replace the same number of individuals randomly selected from current population.

Step 6 (check convergence). If the convergence criteria are met, stop and output the nondominant solutions, Otherwise, return to Step 3. In this IDECell, the convergence criteria are defined as the maximum number of iterations for whole population (G).

5. Numerical Simulation

In this study, the whole optimization period T is set to 8:00–19:00 and divided into 12 sections with the duration T_N of one hour. Besides, it is assumed that there are 100 EVs needed to be charged in the office parking lot.

5.1. Settings of Simulation

(1) Rated Capacity of EV Battery. In the EV market, there are different battery types such as NiMH, Lead Acid, and Li-Ion. According to the Li-Ion battery equipped in "E6 pioneer," EV developed by BYD Co., Ltd., in completely discharging situations, the demand for energy is 60 kW·h.

(2) The Initial SOC of EV Battery. Using probability distribution model to describe the initial SOC of EV battery

$$f\left(\text{SOC}_0, \mu, \sigma\right) = \frac{1}{\sqrt{2\pi\sigma^2}} e^{-(\text{SOC}_0 - \mu)^2/(2\sigma^2)}, \tag{23}$$

where SOC_0 represents the initial SOC of EV battery and it is commonly between 0.05 and 0.5. It takes μ for 0.25 and takes σ for 0.1 and μ is the average value of SOC and σ is standard deviation.

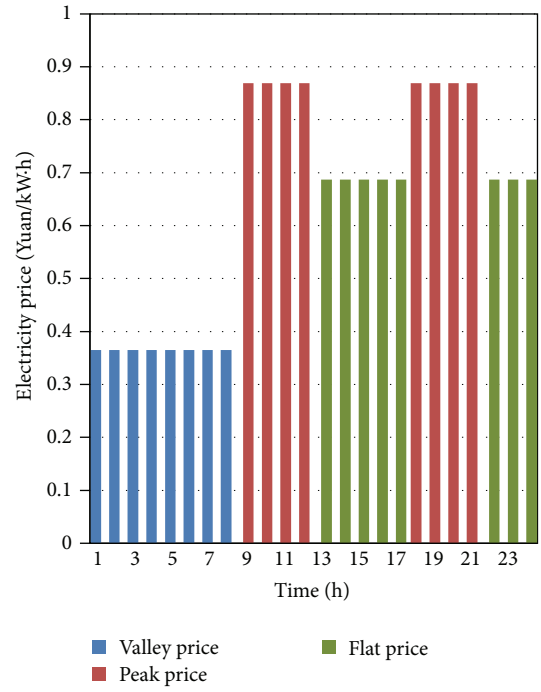

Figure 9: TOU price.

(3) TOU Price. According to actual TOU price implemented in Jiangsu province in China, the period of valley load is defined as 0:00–08:00, totally 8 h; the period of peak load is defined as 09:00–12:00 and 18:00–21:00, totally 8 h. The remaining time is the period of flat load. Adopting the actual price of electricity in the province, the prices of peak, flat, and valley load period are 0.869 Yuan/kW·h, 0.687 Yuan/kW·h, and 0.365 Yuan/kW·h. The histogram of TOU price is shown in Figure 9.

(4) The Daily Output Power of PV Generation. The daily output power of PV generation before regulation can be predicted and the average value per hour of output power is shown in Table 2.

(5) Parameters of IDECell Algorithm. The parameters of IDECell algorithm are set as shown in Table 3.

(6) Typical Charging Pattern of EV Battery. In order to verify the effectiveness of optimized charging strategy which can be obtained by optimization algorithm, adopt a typical charging pattern for comparison, the charging profile of which is consistent with the charging characteristics of battery. At present, the typical strategy for EV battery charging is a two-stage method. The first stage is constant-current charging process which has a constant current and limited voltage and the second stage is constant-voltage charging process which has a constant voltage and limited current. During the whole charging process, most of the charging time would be the first stage in which the charging power has little change. As a result, EV battery could be considered as a constant power load so that the constant-voltage charging process could be

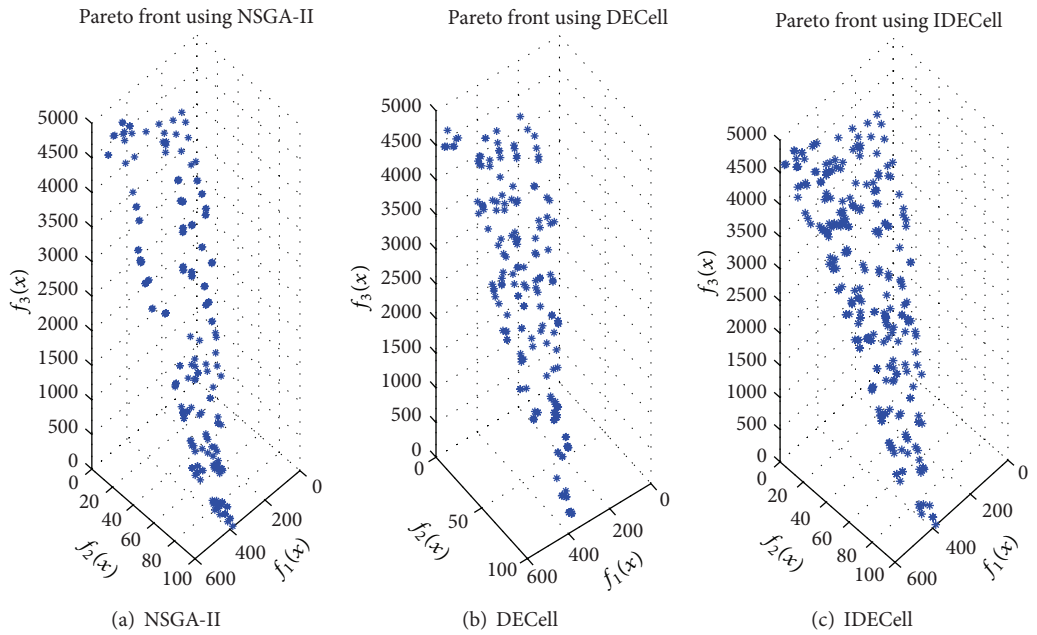

(a) NSGA-II (b) DECell (c) IDECell

Figure 10: Pareto front gained by 3 multiobjective optimization algorithms.

Table 2: Average value per hour of output power of PV generation.

Time (h)	Power (kW)
1	0
2	0
3	0
4	0
5	0
6	9.32
7	82.32
8	479
9	763.68
10	627.32
11	850.04
12	998.68
13	1533.32
14	1446.72
15	1008.32
16	1459
17	1530.32
18	1040.68
19	456.48
20	139.68
21	0
22	0
23	0
24	0

Table 3: Parameters of IDECell algorithm.

Parameter	F	CR	d	P	G	N_D	C
Value	0.8	0.2	10	200	1000	100	20

ignored. In this study, we employ constant power charging way for typical charging pattern.

5.2. The Results and Analysis of Simulation

(1) Performance Comparison of Three Algorithms. Solve the three-objective optimization model established previously using NSGA-II algorithm, DECell algorithm, and IDECell algorithm, respectively, and nondominated solutions could be obtained. The corresponding Pareto fronts are as shown in Figure 10.

It can be seen from Figure 10 NSGA-II algorithm is not applicable to be used to solve the presented three-objective optimization problem in this paper due to its worst convergence and distributivity of three algorithms. Nevertheless, the optimization results gained by DECell algorithm and IDE algorithm are more ideal relatively. Furthermore, compared to the basic DECell algorithm, distribution of the Pareto front gained by the IDECell algorithm has a significant improvement to be more uniform. As a consequence, it is verified that IDECell algorithm is feasible and effective for solving the three-objective optimization model of the coordinated control of PV generation and EVs charging.

(2) Selection of the Optimal Solution. So as to get the best coordinated control strategy of PV generation and EVs charging, it is required to select an optimal solution from the nondominated solution set by a certain method. Thus calculate the normalized value for each nondominated solution of the Pareto solution set according to (24), and then sort them:

$$f_i = \sum_{n=1}^{3} \left(\frac{f_i(n) - f_{\min}(n)}{f_{\max}(n) - f_{\min}(n)} \right), \tag{24}$$

where f_i represents the normalized value of the ith solution; $f_i(n)$ is the fitness value for nth optimization objective

Table 4: Standard deviation under different charging patterns.

Condition	Without EVs	Typical charging pattern	Optimized charging pattern
Standard deviation (kW)	462.14	379.29	277.14
Reduction	—	17.91%	40.02%

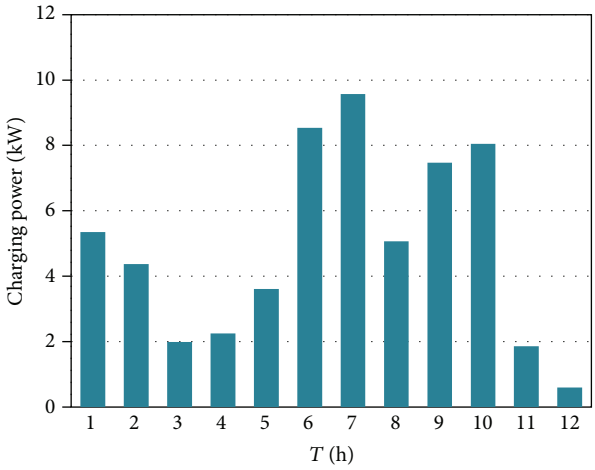

Figure 11: EV charging power for each period.

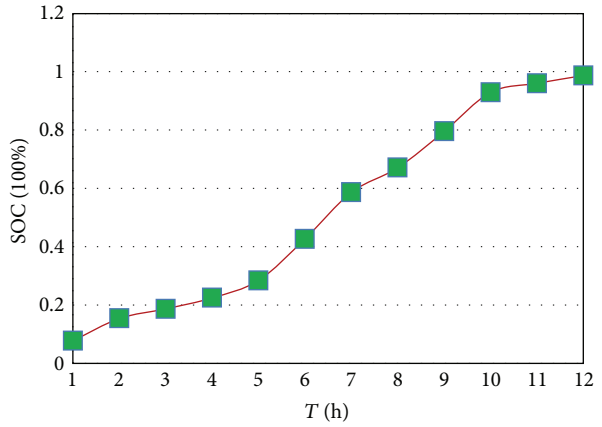

Figure 12: The SOC changing curve of EV battery.

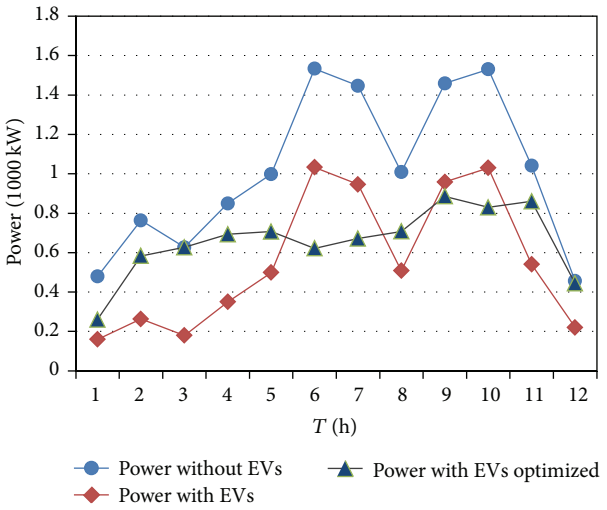

Figure 13: The fluctuation curves of the power transmitted to the grid.

of ith solution; $f_{\min}(n)$ is the minimum fitness value for nth optimization objective of all solutions; $f_{\max}(n)$ is the maximum fitness value for nth optimization objective of all solutions.

On this basis, the solution which has the minimum normalized value can be selected as the optimal solution.

(3) Comparison between the Optimal Charging Pattern and Typical Charging Pattern. As the optimal solution is selected and its corresponding control strategy is considered to be the optimal charging pattern for EVs, the charging power curve of EV battery is as shown in Figure 11. Different from the typical charging pattern, the charging power of the optimal charging pattern changes each period.

According to (6), the SOC of the EV battery can be computed and its changing curve is shown in Figure 12. From Figure 12, the SOC of EV battery is closed to be 100% at the end of the whole optimization period charged by the optimal charging pattern. It is confirmed that the optimal pattern can meet the need of EV charging commendably.

Figure 13 shows the fluctuation curves of the power transmitted to the grid under different conditions; the specific standard deviation values are calculated and shown in Table 4. Both Figure 13 and Table 3 clearly indicate that the optimal charging pattern for EV battery can obviously reduce the fluctuations of the power transmitted to the grid compared to the typical charging pattern.

Figure 14 shows the energy demand of different charging patterns; as it can be seen, the optimized charging pattern can shift a mass of peak load to valley load and flat load which can reduce the charging costs directly.

In addition, Table 5 lists the charging cost of different charging patterns. It is clearly seen that the optimized charging pattern can bring an evident reduction in the cost of EVs charging.

Table 5: Cost under different charging patterns.

Condition	Typical charging pattern	Optimized charging pattern
Cost (Yuan)	4465.6	3977.3
Reduction in cost	—	10.1%

6. Conclusions

The coordinated control of PV generation and EVs charging has been studied. In order to stabilize the fluctuation of

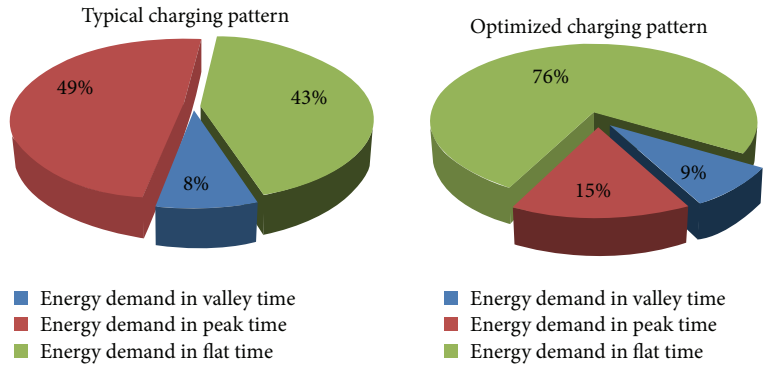

Figure 14: Energy demand of different charging patterns.

the PV generation output power and minimize the total cost for EVs charging while meeting the SOC requirement of EV batteries, a three-objective optimization model is established by controlling the EVs charging power during charging process.

To solve the proposed multiobjective optimization problem effectively, an IDECell algorithm is developed by integrating the meshing method into the DECell algorithm. The modified algorithm is initially successfully applied to solve two benchmark test problems, thus validating the new approach. Compared to NSGA-II and DECell algorithm, IDECell has the best performance in the convergence and uniform distribution according to the simulation results.

With the presented IDECell algorithm, an optimized strategy for coordination control of PV generation and EVs charging has been achieved by a normalization process. Finally, the results of simulations show that the obtained strategy is effective and reliable. Under this strategy, the total cost for EVs charging has been reduced by 10.1%, and the standard deviation of PV generation output also has been decreased to 277.14 kW from 379.29 kW of typical charging pattern.

Conflict of Interests

The authors declare that there is no conflict of interests regarding the publication of this paper.

Acknowledgments

This work is supported by the National High-Tech Research & Development Program of China ("863" Program) (Grant no. 2012AA050210), Provincial Science and Technology Supporting Program (Grant no. BE2011174), and Cooperative Innovation Fund of Industry, Education and Academy of Jiangsu Province (Grant no. BY2014037-29).

References

[1] L. Xu, X. Ruan, C. Mao, B. Zhang, and Y. Luo, "An improved optimal sizing method for wind-solar-battery hybrid power system," *IEEE Transactions on Sustainable Energy*, vol. 4, no. 3, pp. 774–785, 2013.

[2] R.-H. Liang and J.-H. Liao, "A fuzzy-optimization approach for generation scheduling with wind and solar energy systems," *IEEE Transactions on Power Systems*, vol. 22, no. 4, pp. 1665–1674, 2007.

[3] Z. Hu, Y. Song, Z. Xu, Z. Luo, K. Zhan, and L. Jia, "Impacts and utilization of electric vehicles integration into power systems," *Proceedings of the Chinese Society of Electrical Engineering*, vol. 32, no. 4, pp. 1–10, 2012 (Chinese).

[4] U. C. Chukwu and S. M. Mahajan, "V2G parking lot with pv rooftop for capacity enhancement of a distribution system," *IEEE Transactions on Sustainable Energy*, vol. 5, no. 1, pp. 119–127, 2014.

[5] S. Zhang, Z. Hu, Y. Song, H. Liu, and M. Bazargan, "Research on unit commitment considering interaction between battery swapping station and power grid," *Proceedings of the Chinese Society of Electrical Engineering*, vol. 32, no. 10, pp. 49–55, 2012 (Chinese).

[6] N. Rotering and M. Ilic, "Optimal charge control of plug-in hybrid electric vehicles in deregulated electricity markets," *IEEE Transactions on Power Systems*, vol. 26, no. 3, pp. 1021–1029, 2011.

[7] J. Ma and C. N. Nian, "A scheme for renewable grid for EV of 2020 in Chongming island," *Agricultural Equipment & Vehicle Engineering*, pp. 1–7, 2011 (Chinese).

[8] A. Y. Saber and G. K. Venayagamoorthy, "Plug-in vehicles and renewable energy sources for cost and emission reductions," *IEEE Transactions on Industrial Electronics*, vol. 58, no. 4, pp. 1229–1238, 2011.

[9] Z. S. Li, H. B. Sun, and Q. L. Guo, "Study on wind-EV complementation on the transmission grid side considering carbon emission," *Proceedings of the Chinese Society of Electrical Engineering*, vol. 32, no. 10, pp. 41–48, 2012 (Chinese).

[10] D. Yu, S. Song, B. Zhang, and X. Han, "Synergistic dispatch of PEVs charging and wind power in Chinese regional power grids," *Automation of Electric Power Systems*, vol. 35, no. 14, pp. 24–29, 2011 (Chinese).

[11] A. Y. Saber and G. K. Venayagamoorthy, "Resource scheduling under uncertainty in a smart grid with renewables and plug-in vehicles," *IEEE Systems Journal*, vol. 6, no. 1, pp. 103–109, 2012.

[12] D. Y. Yu, H. L. Huang, M. Lei, X. Li, B. Zhang, and X. Han, "CO_2 reduction benefit by coordinated dispatch of electric vehicle charging and wind power," *Automation of Electric Power Systems*, vol. 36, no. 10, pp. 14–18, 2012 (Chinese).

[13] J. Zhao, F. Wen, Y. Xue, Z. Dong, and J. Xin, "Power system stochastic economic dispatch considering uncertain outputs from plug-in electric vehicles and wind generators," *Automation of Electric Power Systems*, vol. 34, no. 20, pp. 22–29, 2010 (Chinese).

[14] G. B. Wang, J. H. Zhao, and F. Q. Wen, "Stochastic optimization dispatching of plug-in hybrid electric vehicles in coordination with renewable generation in distribution systems," *Automation of Electric Power Systems*, vol. 36, no. 19, pp. 22–29, 2012 (Chinese).

[15] X. Q. Zhang, J. Liang, L. Zhang, D. Yu, X. Han, and F. Zhang, "Approach for plug-in electric vehicles charging scheduling considering wind and photovoltaic power in chinese regional power grids," *Transactions of China Electrotechnical Society*, vol. 28, no. 2, pp. 28–35, 2013 (Chinese).

[16] Z. Chen, X. N. Xiao, and X. Y. Lu, "Multi-objective optimization for capacity configuration of PV-based electric vehicle charging stations," *Transactions of China Electrotechnical Society*, vol. 28, no. 6, pp. 238–248, 2013 (Chinese).

[17] K. Deb, A. Pratap, S. Agarwal, and T. Meyarivan, "A fast and elitist multiobjective genetic algorithm: NSGA-II," *IEEE Transactions on Evolutionary Computation*, vol. 6, no. 2, pp. 182–197, 2002.

[18] Z. Wei, Y. x. Feng, J. r. Tan, J. Wu, D. Yang, and J. Wang, "Research on quality performance conceptual design based on SPEA2," *Computers and Mathematics with Applications*, vol. 57, no. 11-12, pp. 1943–1948, 2009.

[19] A. J. Nebro, J. J. Durillo, F. Luna, B. Dorronsoro, and E. Alba, "MOCell: a cellular genetic algorithm for multiobjective optimization," *International Journal of Intelligent Systems*, vol. 24, no. 7, pp. 726–746, 2009.

[20] J. J. Durillo, A. J. Nebro, F. Luna, and E. Alba, "Solving three-objective optimization problems using a new hybrid cellular genetic algorithm," in *Parallel Problem Solving from Nature—PPSN X : 10th International Conference Dortmund, Germany, September 13-17, 2008 Proceedings*, vol. 5199 of *Lecture Notes in Computer Science*, pp. 661–670, 2008.

[21] Y. Zhang, X. D. Zheng, and X. Y. Wan, "Optimization design of hydrodynamic sliding bearing based on differential cellular genetic algorithm," *Journal of Mechanical Transmission*, vol. 38, no. 9, pp. 64–68, 2014 (Chinese).

[22] S. L. Ho, Y. P. Zhao, and W. N. Fu, "An efficient parameterized mesh method for large shape variation in optimal designs of electromagnetic devices," *IEEE Transactions on Magnetics*, vol. 48, no. 11, pp. 4507–4510, 2012.

[23] J. J. Durillo Barrionuevo, *Metaheuristics for Multi-Objective Optimization: Design, Analysis, and Applications*, Universidad de Málaga, 2011.

[24] D. A. van Veldhuizen and G. B. Lamont, "On measuring multiobjective evolutionary algorithm performance," in *Proceedings of the Congress on Evolutionary Computation*, pp. 204–211, July 2000.

[25] E. Zitzler and L. Thiele, "Multiobjective evolutionary algorithms: a comparative case study and the strength Pareto approach," *IEEE Transactions on Evolutionary Computation*, vol. 3, no. 4, pp. 257–271, 1999.